Express Polymer Letters Vol.16, No.7 (2022) 718–734
Available online at www.expresspolymlett.com
https://doi.org/10.3144/expresspolymlett.2022.53

Research article

Influence of UV curing parameters for bio-based *versus* fossil-based acrylates in mechanical abrasion

Pieter Samyn[*], *Joey Bosmans, Patrick Cosemans*

SIRRIS Smart Coating Lab – Department Circular Economy and Renewable Materials, Wetenschapspark 3, B-3590 Diepenbeek, Belgium

Received 31 January 2022; accepted in revised form 27 March 2022

Abstract. The selection of sustainable solutions for protective coatings should consider the use of bio-based materials and environmentally-friendly processing conditions, while their performance needs to be benchmarked against traditional polymer coatings. Therefore, acrylate coatings were formulated by mixing a viscous oligomer (acrylated soybean oil) with a monomer diluent (triacrylate) and applied as a coating on softwood (beech) substrates by curing under ultraviolet (UV) light. In this study, the processing conditions and performance of coatings is explicitly compared by introducing both fossil-based and bio-based grades of the monomer with similar chemical functionality. The wear of coated wood samples was tested on a rotational Taber abrasion tester recording progressive wear loss over 1000 cycles, investigating effects of photoinitiator concentrations and UV curing parameters (light intensity and number of curing passes) on wear resistance. In parallel, the degree of conversion was investigated in relation to other properties such as hardness, water contact angles and topographical evaluation of the wear tracks. Under conditions providing fully cured coatings, the bio-based acrylate coatings systematically present lower wear. This is in agreement with lower hardness and reduced brittleness of the bio-based *versus* fossil-based acrylates. Alternatively, additional insight in the wear properties is obtained from transient wear conditions for partially cured coatings. Most interestingly, the presence of a surface layer with more hydrophobic properties and formation of deposits in the wear track with either island-like or more smooth features was confirmed for the bio-based acrylate coatings, in parallel with the better lubrication and progressive wear reduction. The paper illustrates the benefits in mechanical performance of bio-based coatings when applied under specific processing conditions, which can be implemented at industrial scale in the future, *e.g.*, as protective wood coatings.

Keywords: *thermosetting resins, biopolymers, coatings, mechanical properties*

1. Introduction

Driven by the need of replacing traditional fossil-oil-based polymeric coatings by more sustainable material solutions, industries are eagerly searching for alternative resources based on renewable materials with at least similar performance compared to current state-of-the-art materials. Important aspects of increasing material's lifetime include the surface protection against damage or abrasive wear through the application of high-performance coatings. As such, the combination of bio-based materials for wear protection may allow extending or optimizing the material life-cycle and broaden the circular economy model at both ends, including the material origin and lifetime. Both the selection of renewable materials and/or green processes may contribute to a more sustainable coating design [1], or even outperform traditional synthetic coatings with higher abrasion resistance, stain and sunlight stability [2]. The preservation against degradation and environmental factors of natural surfaces such as wood can be offered by a wide range of coatings depending on the type of required protection, recently including extractives, oils, waxes, resins, biopolymers, and controlled release

[*]Corresponding author, e-mail: pieter.samyn@sirris.be

agents [3]. The use of water-dispersible colloidal lignin particles as a natural wood coating outperforms commercial oil, lacquer, and epoxy coatings based on traditional fossil-based polymers [4]. The bio-based wood coatings may offer excellent properties in hydrophobicity [5], weathering resistance [6], and fire safety [7]. As a specific example, life cycle assessment of UV-curable bio-based coatings for wood indicated that beneficial effects to the environment and health could be created depending on biomass feedstock choice and processing conditions [8]. The mechanical resistance of wood coatings was less investigated, but curable acrylate coatings under ultraviolet (UV) light particularly provide good abrasion and wear protection [9]. The transformation of fossil-based into bio-based materials at industrial level, however, needs practical proof-of-performance in order to make worth investments for adaptation of production processes and/or outperformance is requested to compensate for higher prices of raw materials.

From a viewpoint of incorporating 'green chemistry' principles, bio-based coatings are addressed as suitable candidates for tribological systems requiring ultralow friction or superlubricity [10], including the traditional bio-macromolecules such as chitosan, cellulose and lignin. However, the application of bio-based thermoset resins as bulk materials or coatings directly replacing traditional epoxy or acrylate systems is more suitable for swift industrial implementation. The synthesis of bio-based epoxy resins from cardanol oil and its composites demonstrated high potential for enhancing mechanical and tribological properties [11]. Alternatively, the tribological properties of bio-based acrylate resins were evaluated as a water-soluble bulk polymer after thermal crosslinking, showing improved wear resistance after incorporation of short wood fibers [12]. However, the research and application of bio-based acrylate systems in coating applications for wear protection is rather limited compared to other thermoset polymers, partly also due to the limited industrial access to bio-based acrylic acid and need for the route over lactic acid and their derivatives [13]. Alternatively, bio-based content for the acrylate systems needs to be incorporated into the side-chains connected to the functional acrylate groups. The different routes for synthesis and polymerization of bio-based acrylates were recently reviewed [14]. The incorporation of trifunctional bio-based methacrylates from castor oil was preferred for UV-curable coatings resulting in high crosslinking density and high mechanical resistance [15]. The photocurable acrylates with bio-based monomers indicated higher stiffness and viscosity with increase in the double bond concentration [16]. The processing of bio-based coatings through polymerization under UV light offers benefits for solvent-free handling and gains interest in practical applications [17]. The UV curable acrylate resins typically consist of an acrylate-functionalized oligomer that forms the backbone of the polymer network, mixed with the acrylate monomers that contain small molecules with one to three vinyl groups (*i.e.* mono or multifunctional components). The acrylate formulations are designed with appropriate monomers to adjust the viscosity of the resin and modify the properties of the system [18]. In combination with acrylated soybean oil as an oligomer, the addition of bio-based di-acrylate monomers was screened and resulted in faster photopolymerization rate and reduction in viscosity of the oligomer [19]. The creation of reactive radicals upon irradiation happens through selection of a photoinitiator [20], while the kinetics of the photopolymerization reaction enable fast exothermal curing depending on the UV intensity [21]. A mixture of micro- and macrogels locally forms as a result of the crosslinking between monomers and oligomers, until they percolate into a dense polymer network with final properties depending on the composition and crosslinking degree [22]. The resulting mechanical properties of UV-cured acrylates finally depend on the photopolymerization conditions and crosslinking degree, introducing either more flexibility or brittleness [23]. The visco-elastic features of the polymer network obtained after crosslinking under UV irradiation determine the macroscale deformation properties and mechanical resistance. In particular, the degree of crosslinking is determined by the chemical structure, nature and functionality of both the prepolymers and monomers [24, 25]. The acrylates from cardanol oil were previously used for the production of UV-curable coatings with superior mechanical properties [26]. The polymerization of transparent acrylate or urethane-acrylate coatings under UV irradiation resulted in wear-resistant coatings, which mainly fail due to brittleness and crack growth under fretting [27].

In this work, the role of UV curing conditions on wear resistance of bio-based acrylate coatings is compared to a fossil-based coating with identical

chemical structures. Moreover, the basic influences of processing conditions of bio-based acrylate coatings should be better understood in order to optimize their performance. In particular, the relation between surface properties and wear behavior of bio-based acrylates had not yet been documented. The research question studied herein concerns whether the intrinsic properties of fossil-based and bio-based trifunctional monomers in combination with a selected oligomer offers better wear performance. Indeed, the study provides novel evidence that bio-based alternatives may require slight adaptation in processing parameters or the same processing parameters can provide additional features with improved mechanical performance compared to fossil-based materials.

2. Materials and methods

2.1. Materials

An industrial type of a UV-curable acrylate system was selected, including a multifunctional oligomer (prepolymer) and trifunctional monomer (diluent) with a number of reactive sites per molecule corresponding to the functional acrylate groups (Sarbio, Arkema/Sartomer, Colombes, France). The acrylates with high functionality were used in order to achieve high crosslinking density and appropriate wear resistance. The selected oligomer is derived from bio-based feedstock (*i.e.*, acrylated soybean oil or ASBO) and a comparative study is made with the monomer originating either from biomass (*i.e.*, vegetable oil) or fossil feedstock (*i.e.*, acrylic acid), with chemical structures given in Figure 1a and Figure 1b. The

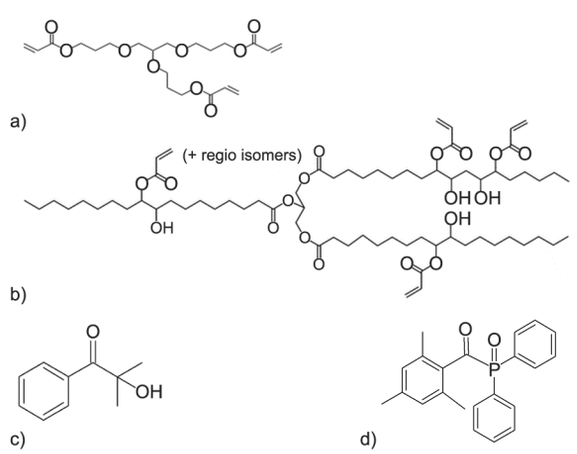

Figure 1. Chemical structures of (a) acrylate monomers (CAS 52408-84-1, purity > 99.9 %), (b) acrylate oligomers (CAS 91722-14-4, purity > 99%; 4-methoxyfenol < 0.5%, triphenylphosphane < 0.25%, phenol < 0.25%), (c) photoinitiator Speedcure 73, (d) photoinitiator Speedcure TPO.

Table 1. Selection of UV-curable acrylate system.

		Bio-based	Fossil-based
Acrylate monomer	**Name**	**Glyceryl propoxy triacrylate**	**Glyceryl propoxy triacrylate**
	T_g	20 °C	20 °C
	η	85 mPa·s	85 mPa·s
	%BRC	14	0
	f	3	3
Acrylate oligomer	**Name**	**ASBO**	N/A[1]
	T_g	20 °C	
	η	20 Pa·s	
	%BRC	0	
	f	4	

[1]Not included in present test matrix.

properties are given in Table 1, including glass transition temperature (T_g), viscosity (η) at 25 °C, functionality *f* and bio-renewable content (%BRC).

The oligomer was mixed with the bio-based and fossil-based monomer in a given weight ratio (wt.) 50/50 wt./wt., together with appropriate photoinitiators (Lambson Ltd., Arkema/Sartomer, Wetherby West Yorkshire, UK). The resin mixture was prepared in a batch of 50 g with slow speed mixing, 300 rpm at 30 °C for 15 minutes. The liquid photoinitiator Speedcure 73 (2-hydroxy-2-methyl-1-phenylpropanone, Figure 1c) provides low yellowing and high surface cure with a maximum absorption at 244 nm, while the powdery Speedcure TPO (2,4,6-trimethylbenzoyldiphenylphosphine oxide, Figure 1d) provides high reactivity and better depth cure with absorption at 267, 298 and 380 nm. The photoinitiator mixture Speedcure TPO/Speedcure 73 was used in a ratio 1/2 wt./wt., as suggested, to provide a good ratio between surface and bulk curing.

2.2. Coating application and UV curing conditions

The coating was manually applied through a bar coating onto softwood substrates (beech, *Fagus sylvatica*) with planed and sanded top surface, resulting in a wet film thickness of 70 µm. The wood substrates were primarily dried overnight in a hot-air oven at 60 °C in order to balance the moisture content. The coatings were subsequently cured after application in an automated UV curing system Aktiprint T/e (Technigraf, Grävenwiesbach-Hundstadt, Germany), containing a mercury (Hg) lamp with selected intensity of 60 or 220 W/cm^2 and constant transport band velocity at 7 m/min and 30 mm lamp-to-belt distance. The number of passes under the UV

Table 2. Test matrix with coating compositions (per batch) and UV curing conditions.

Parameter		Value
Monomer content	[g]	25 (bio-based) or 25 (fossil-based)
Oligomer content	[g]	25 (bio-based)
Speedcure TPO content	[g]	0.5 1.0 2.0
Speedcure 73 content	[g]	1.0 2.0 4.0
UV light intensity	[W/cm^2]	60 220
Number of UV curing passes		1 3 5 10

lamp was stepwise increased from 1 to 10 in order to achieve different degrees of curing. The testing matrix including different coating compositions and curing conditions is summarized in Table 2. For clarity, the compositions with bio-based monomer and bio-based oligomer are referred to as '*bio-based coating*', and the compositions with fossil-based monomer and bio-based oligomer are referred to as '*fossil-based coatin*g'. The processing conditions are intentionally chosen to result in both fully-cured or partially-cured coatings. The solvent resistance after curing of the coatings was assessed according to the methyl ethyl ketone (MEK) scrub test described by the American Society for Testing and Materials (ASTM D 4752) registering the number of double rubs with a soaked cotton cloth to cause coating mar and breakthrough (*i.e.*, exposure of the wood substrate), which can be considered as an equivalent for the curing state of the coating.

2.3. Characterization

The chemical conversion of monomers and oligomers during UV curing was characterized by attenuated total reflection Fourier transform infrared spectroscope (ATR-FTIR), using a Spectrum 65 spectrometer with diamond crystal (Perkin Elmer, Rodgau, Germany). The set-up typically provides chemical information on the top 20 µm underneath the surface, which is appropriate in the present case to identify the bulk properties of coatings with a (wet) thickness of around 70 µm.

Abrasive wear tests on coated wood samples were performed on a circular Taber tester type Model 5135 (Taber Industries, North Tonawanda, New York, USA) according to ASTM D4060-10: abrasion resistance of organic coatings by the Taber abrader. The coated substrates were mounted on a horizontal table with rotational speed of 72 rpm and in contact with a pair of pivoted arms to which two abrasive wheels were attached under a load of 250 g. The abrasive wheels were CS-10 Calibrase types (Shore hardness D = 29) consisting of aluminum oxide particles embedded in a resilient rubber matrix. The wheels were conditioned against a S-11 resurfacing disc each time before loading a new test sample (*i.e.*, after 1000 cycles). The abrasive wear is reported as cumulative weight loss measured on an analytical balance with accuracy of 0.0001 g (Sartorius, Göttingen, Germany) at specified number of cycles N = 250, 500, 750 and 1000 as determined in ASTM D4060-10. The Taber index T is alternatively defined as the weight loss per number of testing cycles N = 1000. From preliminary testing, accurate weight loss of the worn coating was possible to determine in parallel with the relatively small weight of the initial samples (about 30 g sample and 7 g coating). The abrasive tests were repeated on three independent samples and reported as average values.

Hardness of coated samples was determined with a handheld microhardness tester or Shore D durometer (Elcometer, Nieuwegein, The Netherlands) according to ASTM D2240: Standard test method for durometer hardness. The hardness was measured through indentation of a hardened steel tip with a 30±0.5° conical point and 0.100±0.012 mm tip radius, while recording the indicated reading within 1 s after the presser foot is in contact with the specimen. Reported values are averaged over 10 independent measuring locations. Contact angles of static water droplets (3 µl) are measured on an optical contact angle goniometer type OCA 50 (DataPhysics, Filderstadt, Germany) and averaged over 10 locations, using a tangent fitting procedure.

The morphology of the wear tracks was first analyzed through optical microscopy by using a stereomicroscope at magnifications 8× and 50× (Leica, Wetzlar, Germany). The topography of the wear track was further visualized by confocal scanning microscopy type VK-X3000 at a magnification of 10× (Keyence, Mechelen, Belgium), showing a laser image and topographical height image.

3. Results and discussion

3.1. Coating formulations and curing conditions

In relation to the applied conditions of UV curing and photoinitiator concentrations, the coatings with various degrees of crosslinking were intentionally obtained. An overview on the evaluation of the chemical scrub tests with MEK leading to breakthrough of

the coatings with bio-based monomers and oligomers is given in Figure 2, including different curing conditions with photoinitiator content and number of passes. The coating resistance in a solvent scrub test is expressed as the number of double rubs leading to full removal of the coating. As this is a measure of the solvent resistance for the coating, it can be considered that a higher number of rubs is equivalent to a higher degree of crosslinking within the polymer network [28]. The coatings with a number of double rubbing cycles above 200 can be considered in the fully-cured state comparable to other reports of acrylate resins [29], which are not further detailed in the graph to prevail enough detail for the partially-cured samples. These conditions were confirmed as they developed a tack-free coating. The results for bio-based coatings are presented and very similar to the results for fossil-based coatings within a maximum error of 5 double rubs. Given the similar functionality and chemical structure of bio-based and fossil-based monomers, it can be concluded that the curing properties of both alternatives are not affected by their origins. The observations suggest similar reactivity and curing kinetics of both the bio-based and fossil-based coatings, resulting in a crosslinked polymer network with chemical solvent resistance. In particular, the degree of curing evidently increases with photoinitiator concentration, number of passes, and higher UV power ranging from 60 W/cm^2 (Figure 2a) to 220 W/cm^2 (Figure 2b).

An example of the ATR-FTIR spectrum for a non-cured and cured sample with bio-based monomer and oligomer (*e.g.*, 60 W/cm^2, 1 g Speedcure TPO + 2 g Speedcure 73, 5 passes) is illustrated in Figure 3a. The peaks characteristics for functional groups in acrylate monomers and polymers are recognized [30], most prominently related to the presence of ester bonds near 1720 cm^{-1} (C=O stretching), ether

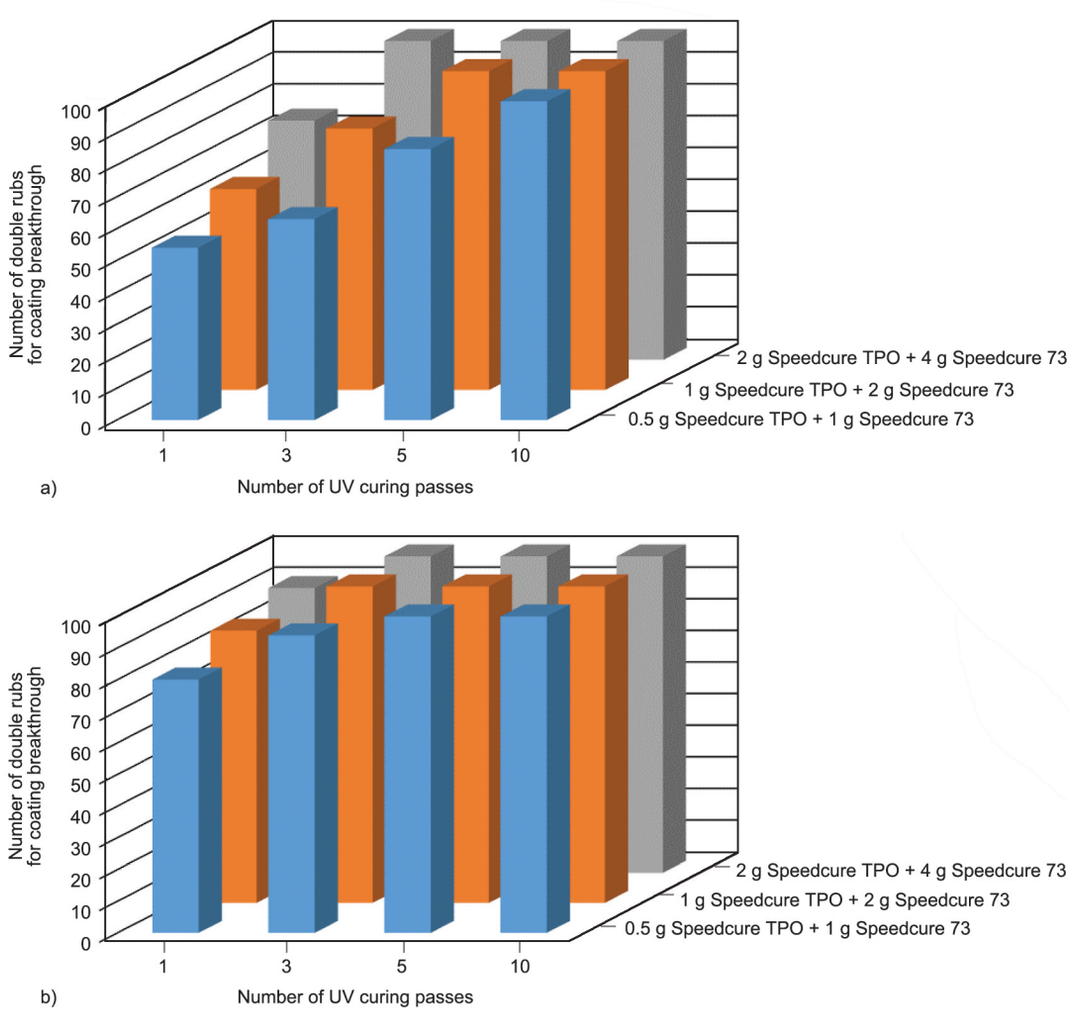

Figure 2. Evaluation of solvent scrub test with MEK of bio-based coatings obtained under different conditions of photoinitiator concentration and number of curing passes for a UV power of (a) 60 W/cm^2, or (b) 220 W/cm^2.

bonds at 1050 to 1230 cm^{-1} (C–O–C stretching) and reactive vinyl groups. The spectra can be used for evaluation of the photochemical crosslinking reaction and curing kinetics of the acrylate coating in presence of photoinitiators and for different curing conditions, depending on the conversion of acrylate bonds [31]. The UV curing induces a polymerization reaction near the C=C double bonds of the reactive monomers [32], as indicated by a decrease in the intensities near 1630 cm^{-1} (C=C stretching), 1405 cm^{-1} (=C–H deformation) and 810 cm^{-1} (=CH_2 twisting). The band at 1240 cm^{-1} for the cured sample is characteristic of the formation of an ester O=C–O–C bond in the polymerized acrylate. The latter also induces conformational changes in the ordering of C–O–C bonds as represented in a small shift of the ether groups from 1188 to 1156 cm^{-1}. The percent of conversion of the C=C bonds can be calculated from the relative intensities I of the band at 810 cm^{-1} *versus* 1730 cm^{-1} before curing $(I_{830}/I_{1730})_0$ and after curing $(I_{830}/I_{1730})_c$, according to Equation (1) [33]:

$$Conversion\,[\%] = \frac{\left(\frac{I_{810}}{I_{1730}}\right)_0 - \left(\frac{I_{810}}{I_{1730}}\right)_c}{\left(\frac{I_{810}}{I_{1730}}\right)_0} \cdot 100 \qquad (1)$$

The monomer conversion for different curing conditions is quantified in Figure 3b, obviously giving higher conversion with increasing power, higher photoinitiator concentration and increasing number of passes. The most important parameters to achieve appropriate final conversion of UV cured materials are the light intensity and irradiation time, while the photoinitiator concentration can mainly influence the initiation of the conversion at low number of curing passes related to the number of reactive locations. In that respect, the conversion during photopolymerization of coatings with fossil-based and bio-based monomers follows the same trend under comparable curing conditions, which confirms similar reactivity of the coating grades in parallel with their identical chemical structure and functionality. The conversion rate obviously is high during the first number of curing passes, while it gradually slows down as the conversion increases. In general, a relatively high degree of conversion up to 90% can be achieved after sufficient reaction time, but full conversion of 100% does not exist as a so-called gel point is reached after a relatively fast increase in the conversion during the first number of curing passes. The progressive increase in viscosity during photochemical crosslinking

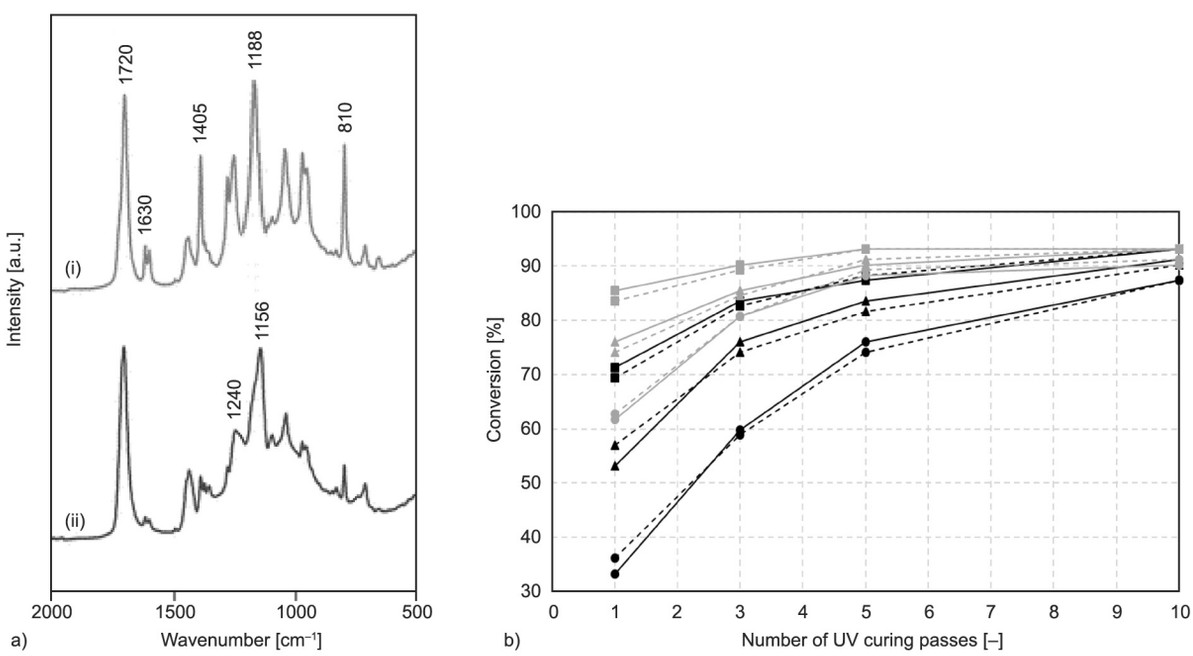

Figure 3. UV photocuring of acrylate monomers and oligomers (a) detail of the ATR-FTIR spectrum for (i) uncured coating and (ii) cured coating under 60 W/cm^2, 1 g Speedcure TPO + 2 g Speedcure 73, 5 passes, (b) conversion of fossil-based acrylate monomers and oligomers (full-line) and bio-based acrylate monomers and oligomers (dotted line) under different conditions with power 60 W/cm^2 (black lines) and 220 W/cm^2 (grey lines) with different photoinitiation content, (●, ●) 0.5 g Speedcure TPO + 1 g Speedcure 73, (▲, ▲) 1 g Speedcure TPO + 2 g Speedcure 73, (■, ■) 2 g Speedcure TPO + 4 g Speedcure 73.

of the polymer network inhibits high mobility of the monomer chains and reduces diffusion of the free radicals, which restricts the complete crosslinking. As a reference test, a conversion of around 78% was obtained for the pure oligomer, while the mixtures of oligomer with a compatible monomer obviously may reach higher conversion levels at around 90 % in parallel with the reduced viscosity and higher mobility of the polymer structure upon addition of the monomer [28]. The high conversion for the present system could be expected because of the high functionality, relatively low viscosity and high efficiency of the selected photoinitiators for the selected monomers. In parallel with the relatively high conversion, good adhesion with the wood substrate remained existing for the present coating compositions in contrast with other systems [34], likely due to the high T_g and flexibility of the selected monomer and oligomer. A remaining fraction of 5 to 10% of non-reacted acrylate groups is generally in line with previous analysis of gel fraction analysis [35], which might affect mechanical properties as illustrated below. In conclusion, the photochemical crosslinking of bio-based and fossil-based coatings follows similar kinetics depending on the light intensity, photoinitiator concentrations and number of curing passes.

3.2. Abrasive wear testing of bio-based *versus* fossil-based acrylate coatings

The abrasive wear loss of the acrylate coatings was evaluated for compositions with either bio-based or fossil-based monomers, including different UV curing parameters and photoinitiator concentrations. Both conditions for fully cured coatings (*i.e.*, referred to as steady-state wear conditions) and partially cured coatings (*i.e.*, referred to as transient wear conditions) were intentionally studied in order to get better insight into the influence of curing conditions and intrinsic properties of the coatings with bio-based *versus* fossil-based monomers. The wear measurements were undertaken almost immediately after curing in order to avoid additional environmental effects or further curing.

The results for steady-state abrasive wear conditions of fully cured coatings are shown in Figure 4 and were obtained for compositions with the highest photoinitiator concentration (2 g Speedcure TPO + 4 g Speedcure 73) in combination with both UV irradiation intensities (60 or 220 W/cm^2). The wear results are reported as an average weight loss at given number of wear cycles, and the statistical variation has been determined on the final reading of abrasive wear loss after 1000 cycles. Due to the sensitivity of the Taber abrasive wear testing depending on many parameters, an acceptable statistical variation on weight loss is typically reported in the range of 10 to 15% [36], and an acceptable range of 7 to 10% statistical variation has thus been obtained in the present study. The statistical variation obviously becomes lower as the curing of the coatings is more complete, likely because the crosslinking density over the coating also becomes more homogeneous. The fully cured coatings with higher photoinitiator content provide lowest wear rates compared to the coatings with lower photoinitiator content, in parallel with the conditions of a fully crosslinked polymer network. The increase in number of curing passes evidently reduces the wear as the crosslinking reaction between monomer and oligomers proceeds with irradiation time through a radical process under UV curing. The crosslinking density of the polymer network consequently increases with number of passes, which results in the higher mechanical resistance. The increase in UV light intensity causes a further reduction and wear and frequent stabilization in performance after a smaller number of processing steps. In particular, the coatings with bio-based monomers present lower wear compared to the fossil-based analogues under comparable curing conditions. This evolves as a remarkable intrinsic property of the coatings with bio-based monomers, as the conversion of bio-based coatings was determined to be similar to the fossil-based coatings. In conclusion, the comparable photochemical conversions for bio-based and fossil-based coatings result in lower abrasive wear for bio-based coatings. Whereas the bulk properties related to the crosslinking density are thus comparable, the observations of wear resistance are further explained in parallel with evaluation of the physicochemical surface properties, as below.

The results for transient wear performance of partially cured coatings are shown in Figure 5 and interestingly reveal differences in intrinsic properties of bio-based *versus* fossil-based coatings. Although the wear losses of partially cured coatings have inherently some higher statistical variations of 9 to 12%, consistent trends can be recognized. The lower photoinitiator concentrations provide irregular performance as expected for acrylate coatings with lower degree of crosslinking. The presence of remaining

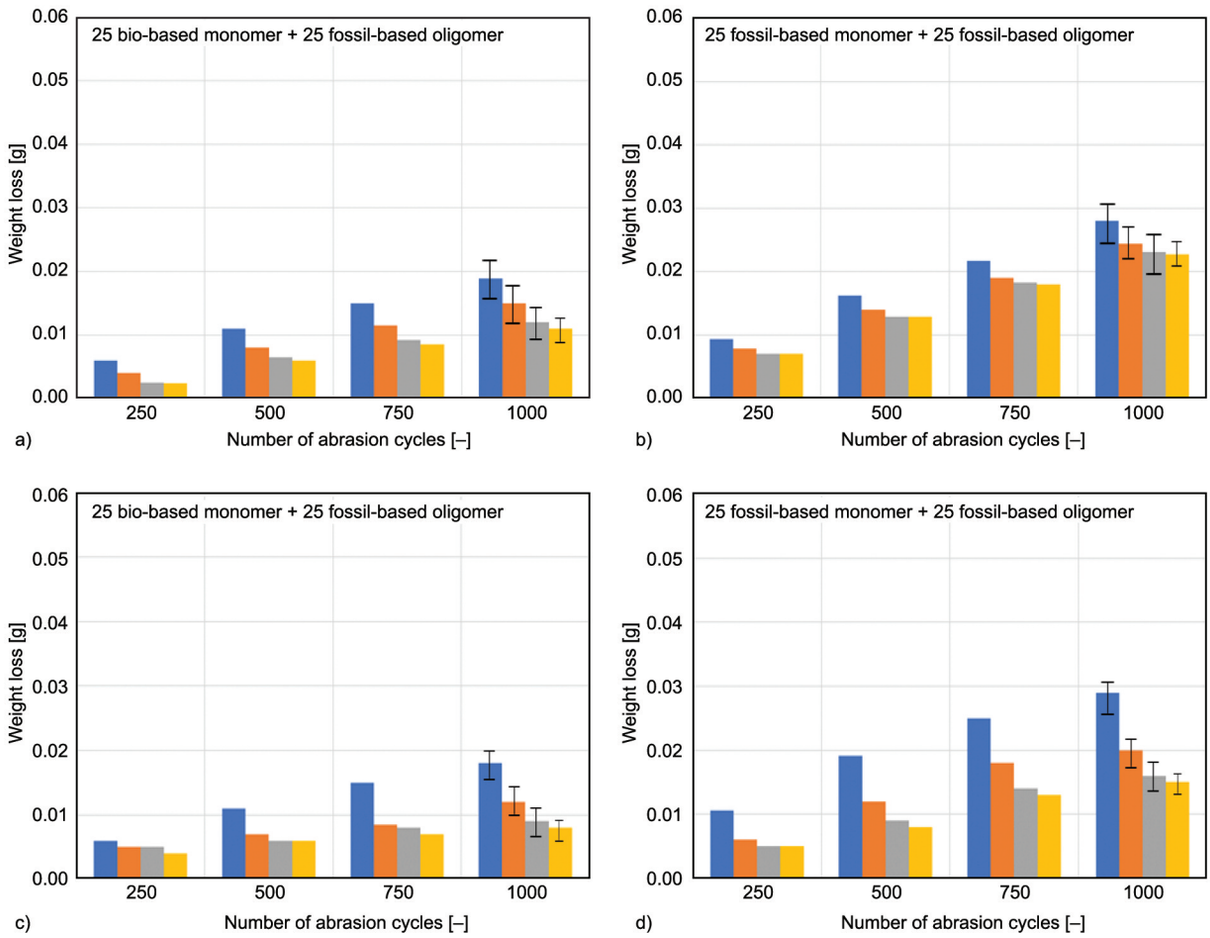

Figure 4. Steady-state abrasive wear for fully UV-cured bio-based and fossil-based acrylate coatings: cumulative weight loss as a function of abrasion cycles indicating the influence of curing intensity, *i.e.* (a, b) 60 W/cm^2, (c, d) 220 W/cm^2, and increasing number of UV curing passes represented by the subsequent bars, *i.e.* (i) 1 (blue), (ii) 3 (orange), (iii) 5 (grey), (iv) 10 (yellow) – fixed photoinitiator 2 g Speedcure TPO + 4 g Speedcure 73.

monomer fractions may strongly interfere with the abrasion depending on the balance between mechanical strength of the polymer network *versus* eventual lubricating activity of the monomer fraction. The number of curing passes consequently has an influence on the wear resistance, but significant differences are observed for bio-based *versus* fossil-based coatings. Most interestingly, the evolution of wear for fossil-based acrylates with number of curing steps increases after small number of curing steps and only decreases upon sufficient curing, which is not observed for the bio-based coatings. The presence of a residual monomer fraction might have a more prominent effect in fossil-based compared to bio-based coatings and gives an indication for different curing kinetics between bio-based and fossil-based components. The effect of a residual monomer fraction in partially cured coatings depends on the balance between mechanical strength and lubricity: it seems to have dominant lubricating properties for the bio-based coatings while dominantly causing insufficient mechanical strength for fossil-based coatings. The effects of a residual monomer content are further confirmed below by means of hardness measurements and water contact angles.

3.3. Hardness testing of bio-based *versus* fossil-based acrylate coatings

The measurement of microhardness values is most widely applied to characterize mechanical resistance of cured coatings on wood substrates, as it provides better sensibility compared to alternative measurements such as a pendulum hardness test or pencil hardness [37]. The results for microhardness of bio-based and fossil-based coatings with different photoinitiator concentrations and curing conditions at 60 or 220 W/cm^2 are given in Figure 6. Statistical variation in the microhardness is somewhat higher for the partially cured samples and becomes within a standard deviation of ±2 units for the fully cured

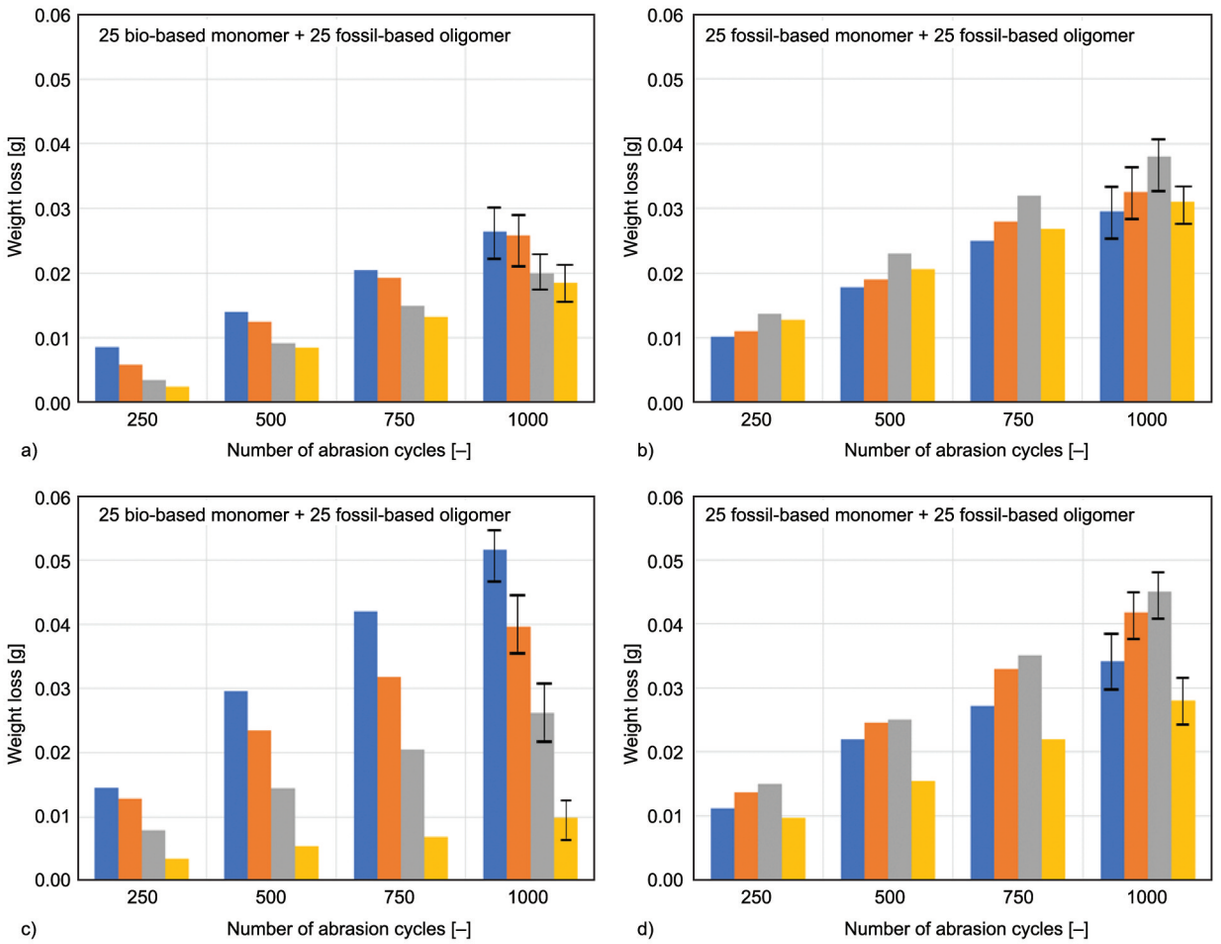

Figure 5. Transient abrasive wear for partially UV-cured bio-based and fossil-based acrylate coatings: cumulative weight loss as a function of abrasion cycles indicating the influence of photoinitiator concentration, *i.e.* (a, b) 0.5 g Speedcure TPO + 1 g Speedcure 73, (c, d) 1 g Speedcure TPO + 2 g Speedcure 73, and increasing number of UV curing passes represented by the subsequent bars, *i.e.* (i) 1 (blue), (ii) 3 (orange), (iii) 5 (grey), (iv) 10 (yellow) – fixed UV light intensity 60 W/cm^2.

samples. The hardness of the acrylate coatings mainly depends on the flexibility of the polymer chains and crosslinking density of the coating [38]. Therefore, it is evident that an increase in hardness is measured with increasing number of curing passes and higher photoinitiator concentrations as the conversion of double bonds progressively increases within the formation of a more densely crosslinked polymer network. Overall, there is a remarkable trend that the hardness of bio-based coatings is lower than for the fossil-based analogues. Although molecular structure, functionality and conversion of biobased and fossil-based coatings are similar, the hardness properties of the bulk coatings may depend on the formation of micro- to nanoscale organized structures. The local inhomogeneities in coating structures obtained by the photopolymerization of multifunctional acrylates were studied by XRD [39], illustrating the existence of microgel clusters with different sizes. In particular, the local ordering on agglomerated microgel structures was frequently studied and can be considered as the existence of hard nanocrystalline regions within an amorphous matrix [40]. The latter was expected to develop mainly for highly crosslinked systems, where it is supposed that highly crosslinked zones are embedded into a less crosslinked matrix [41]. The latter microstructure was proved to result in a lower elasticity and higher ductility of the bio-based acrylate network [42]. These mechanical properties are in line with the lower abrasive wear bio-based coatings under steady-state curing conditions. As most important conclusion, the bio-based coatings are consequently more ductile and resistant to abrasion, while the fossil-based coatings are more brittle and sensitive to abrasion.

The increase in hardness of a coating is generally seen as a key factor that improves the mechanical abrasion resistance. For the present system, however,

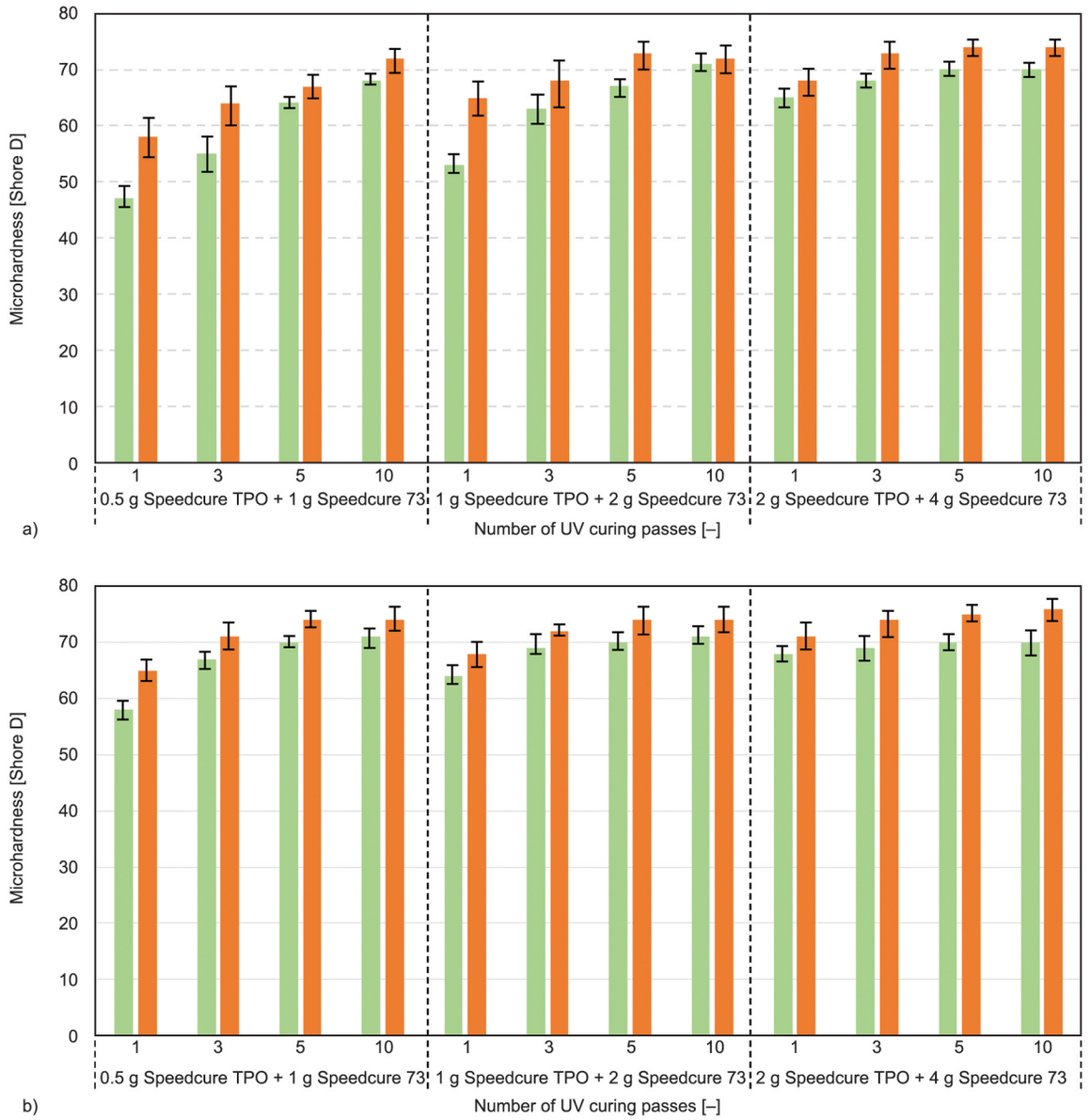

Figure 6. Hardness of UV-cured acrylate coatings with different composition of 25 bio-based monomer + 25 fossil-based oligomer (green bars), or 25 fossil-based monomer + 25 fossil-based oligomer (orange bars), including different UV curing conditions with photoinitiator concentrations and UV curing passes (1, 3, 5, 10) at (a) 60 W/cm^2, and (b) 220 W/cm^2.

the systematic increase in hardness with more severe curing conditions may not be fully in parallel with the changes in abrasive wear. In particular, the transient wear conditions indicate a discontinuous trend in wear resistance that is not observed in hardness. The relationships between hardness, conversion and abrasive wear loss are illustrated in Figure 7 for conditions of steady-state wear (no transient wear conditions included in the graphs). As expected, the increase in hardness evolved with an increase in conversion degree in the photopolymerized acrylate network, but a different trend with lower wear of bio-based *versus* fossil-based coating is in line with the before mentioned structural details (Figure 7a). In parallel, the relationships between Taber index T with conversion (Figure 7b) and hardness (Figure 7c) illustrate a decreasing trend confirming the role of the intrinsic mechanical properties on wear properties, *i.e.* the higher abrasive wear resistance is obtained with an increase in mechanical properties. However, the latter trends are different for bio-based and fossil-based coatings as the mechanical properties indeed refer to the bulk properties of the coatings. In parallel, the lack of relationship between hardness and abrasive wear under transient conditions confirms that the wear properties are highly determined

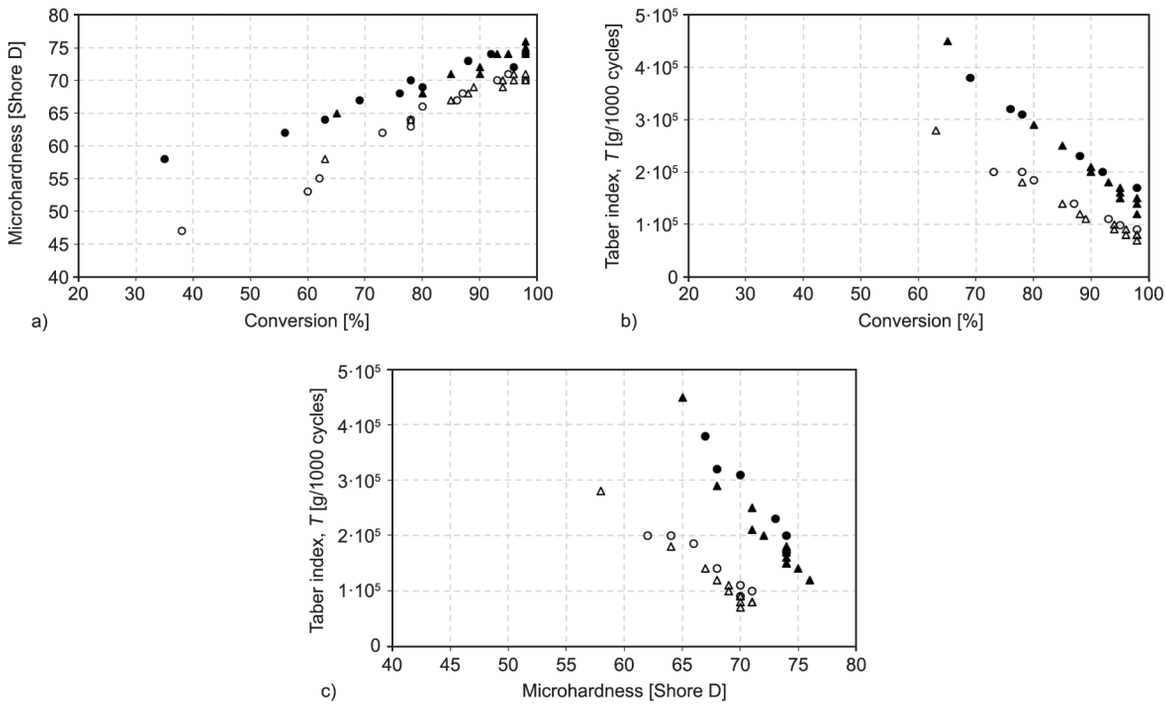

Figure 7. Relationship between intrinsic mechanical properties and abrasive wear resistance for bio-based coatings (open symbols ○ 60 W/cm^2, Δ 220 W/cm^2) and fossil-based coatings (closed symbols ● 60 W/cm^2, ▲ 220 W/cm^2), (a) microhardness *versus* conversion, (b) Taber index *versus* conversion, (c) Taber index *T versus* microhardness.

by presence of a non-converted or residual monomer fraction that determines the surface properties. The latter fraction may indeed be enriched at the surface in combination with the possible migration of non-polymerized monomers towards the surface [43], resulting in surface properties that are different from the bulk properties relating to the coating hardness. The presence of this soft surface layer can indeed be confirmed through the solvent scrub tests before.

3.4. Contact angles of bio-based *versus* fossil-based acrylate coatings

As the abrasive wear properties strongly relate to the chemical surface composition, as concluded before, the differences between bio-based *versus* fossil-based coatings are further studied in relation with the static water contact angles, as presented in Figure 8. The water contact angles are measured immediately after deposition of the water droplet and thus represent initial contact with the eventual build-up of a surface layer on the coating. Typical standard deviation of static water contact angles is around ±2°. The water contact angles confirm that the bio-based coatings are more hydrophobic than fossil-based coatings under all curing conditions. In particular, the contact angles remain relatively constant for the fully cured coatings with high concentration of photoinitiator (*i.e.*, 90° for bio-based coatings and 85° for fossil-based coatings), but stronger variations in hydrophobicity are noticed for the partially cured coatings that visually have a more viscous-like liquid coverage of the surface. Indeed, a common trend occurs that the water contact angle is relatively higher for the weakly cured coatings, while it gradually decreases with the higher number of curing steps until stabilizing at an intermediate value for the fully cured coating. This trend indicates that a residual monomer layer remains present at the surface for the partially cured coatings, which obviously gradually disappears with increasing curing passes. In relation with previous wear data, the more hydrophobic surface layer for bio-based coatings may provide better lubricity compared to fossil-based coatings. In conclusion, the benefits of higher wear resistance for the bio-based coatings may be related to the lubricating properties of a residual monomer layer with more hydrophobic properties compared to fossil-based coatings.

3.5. Microscopic evaluation of wear tracks

The optical aspect of the wear tracks for a fully cured fossil-based and bio-based coating is illustrated in Figure 9. The fossil-based coatings are characterized by a clearly shaped wear track indicating strong

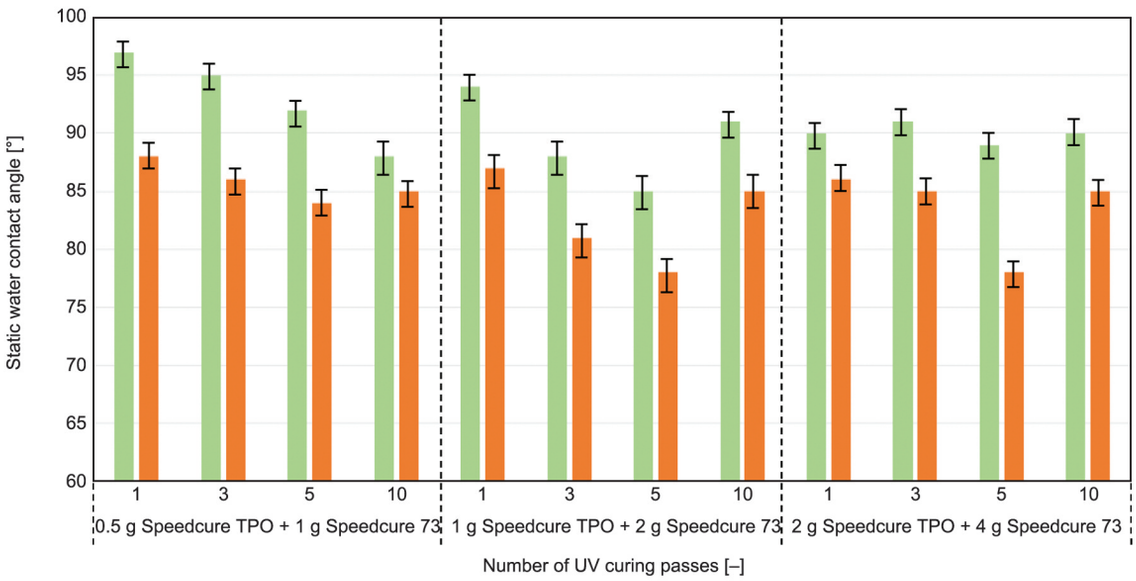

Figure 8. Water contact angles of UV-cured acrylate coatings with different composition of 25 bio-based monomer + 25 fossil-based oligomer (green bars), or 25 fossil-based monomer + 25 fossil-based oligomer (orange bars), including different UV curing conditions with photoinitiator concentrations and UV curing passes (1, 3, 5, 10) at 60 W/cm^2.

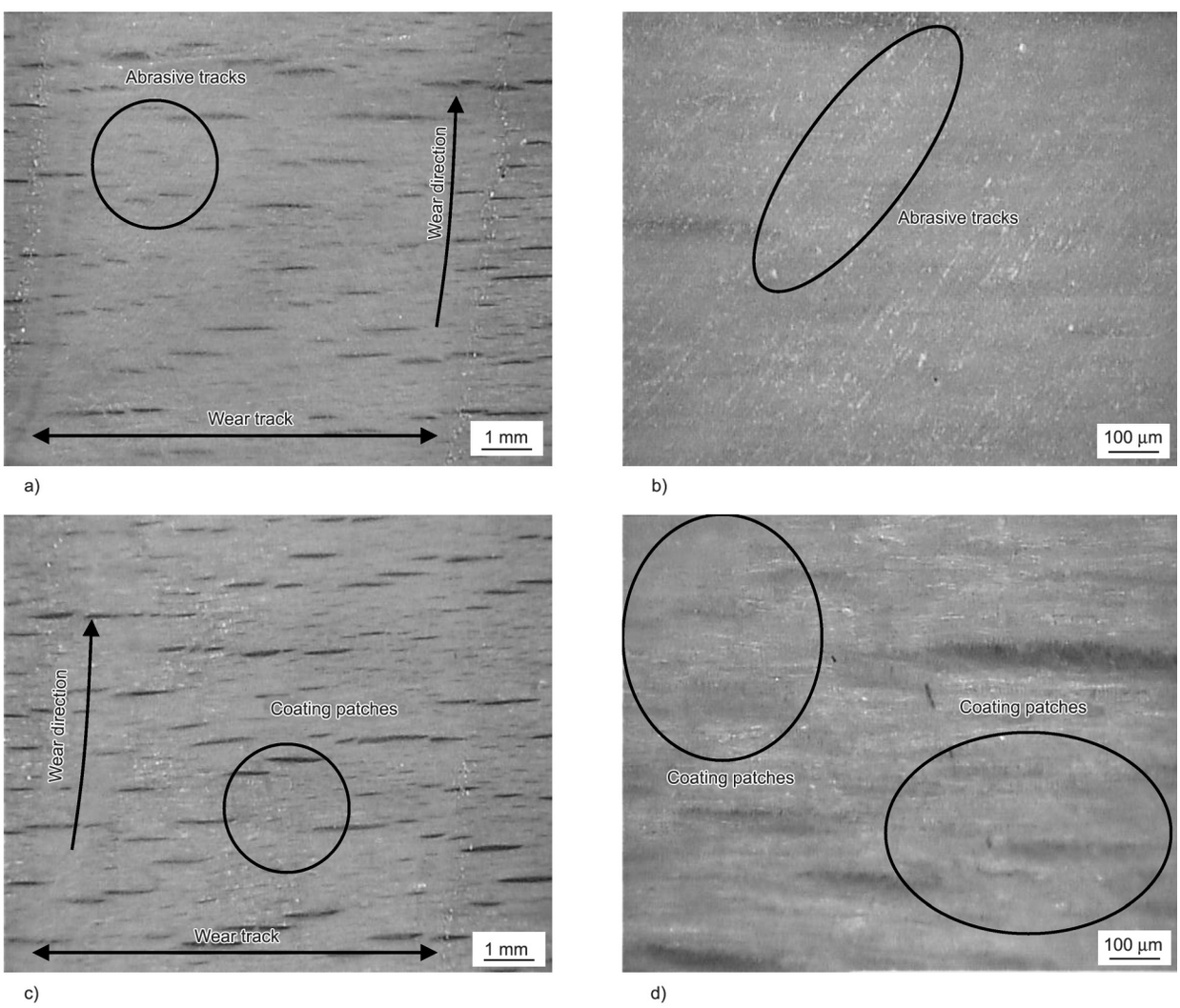

Figure 9. Optical microscopy of abrasive wear tracks of acrylate coatings on wood substrate at magnifications 8× and 50×, (a, b) fossil-based coating, (c, d) bio-based coating under full curing conditions (*e.g.*, 10 curing passes at 60 W/cm^2 with 2 g Speedcure TPO + 4 g Speedcure 73).

abrasive wear tracks. In contrast, the bio-based coatings have a more irregular wear track with the more ductile deformation and remaining island-like patches within the wear track. These observations are in agreement with the previous microhardness measurements, indicating the harder and more brittle behavior of the fossil-based coatings in contrast with the lower hardness and more ductile behavior of the bio-based coatings. The higher intrinsic ductility of bio-based materials favorably induces deformation within the wear track, leading to the lower abrasive wear sensitivity.

A detailed evaluation of the wear tracks for fossil-based coatings with different curing conditions is

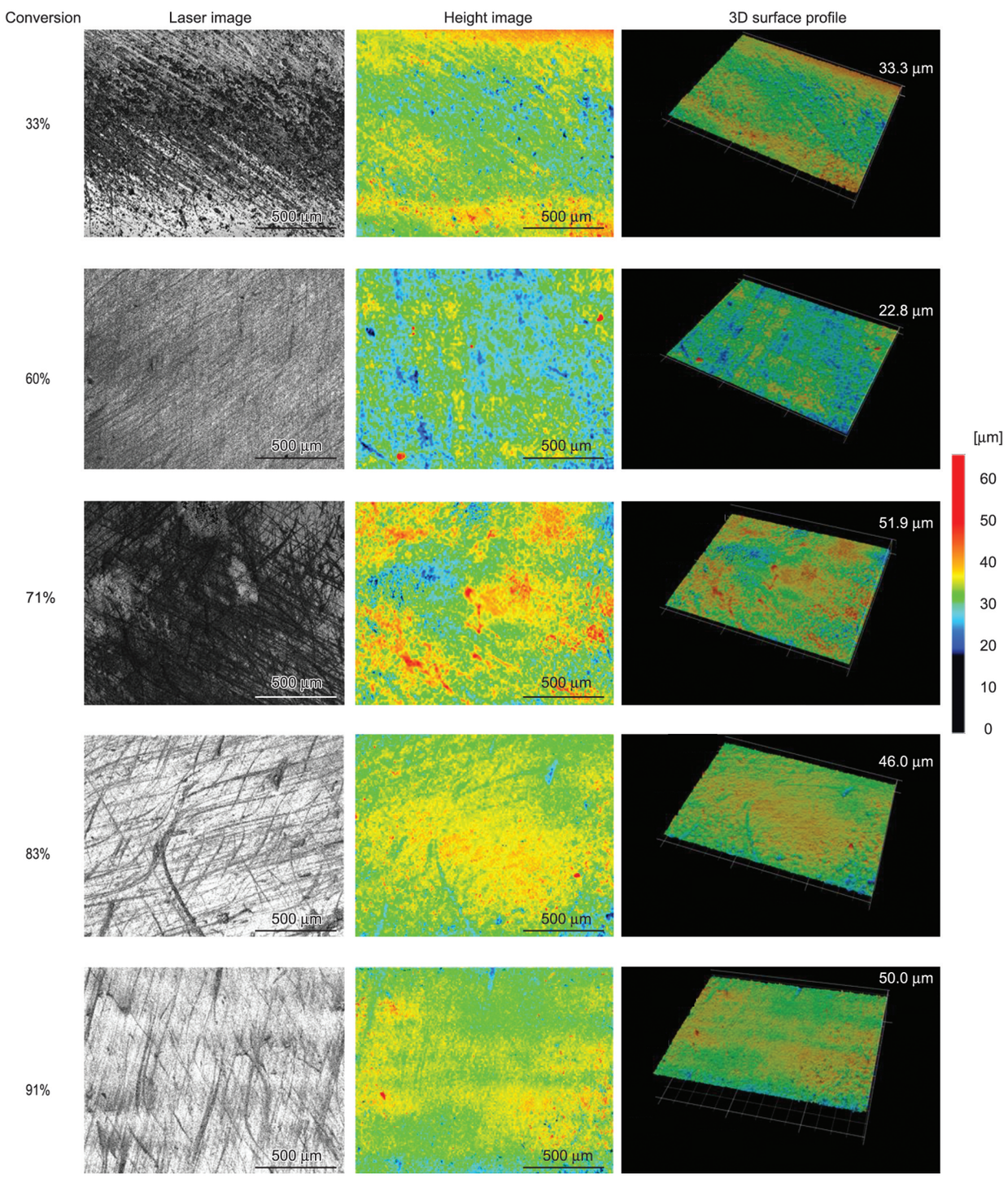

Figure 10. Topographical evaluation of the wear tracks for fossil-based coatings with increasing degree of conversion (60 W/cm^2), including laser image, height image and 3D surface profile (all surface areas are 1000×1500 µm^2 taken at magnification 100×, number on 3D scan represents max *z*-scalescans).

shown in Figure 10. A selection of curing conditions at fixed intensity 60 W/cm^2 is represented, corresponding to increasing degree of conversion depending on number of passes or photoinitiator concentrations. In all cases, severe abrasive wear tracks are observed as grooves that are randomly oriented due to the rotational motion of the abrasive wheels. The severe wear tracks are worn out at different degree depending on the curing conditions. For the weakest curing conditions and consequently lowest degree of conversion, most of the coating is centrally worn and the wood substrate becomes almost visible. With increasing degree of conversion, irregular wear of the coating is observed with deep abrasive grooves. The surface profiles indicate a brittle wear aspect with protrusions in between the abrasive

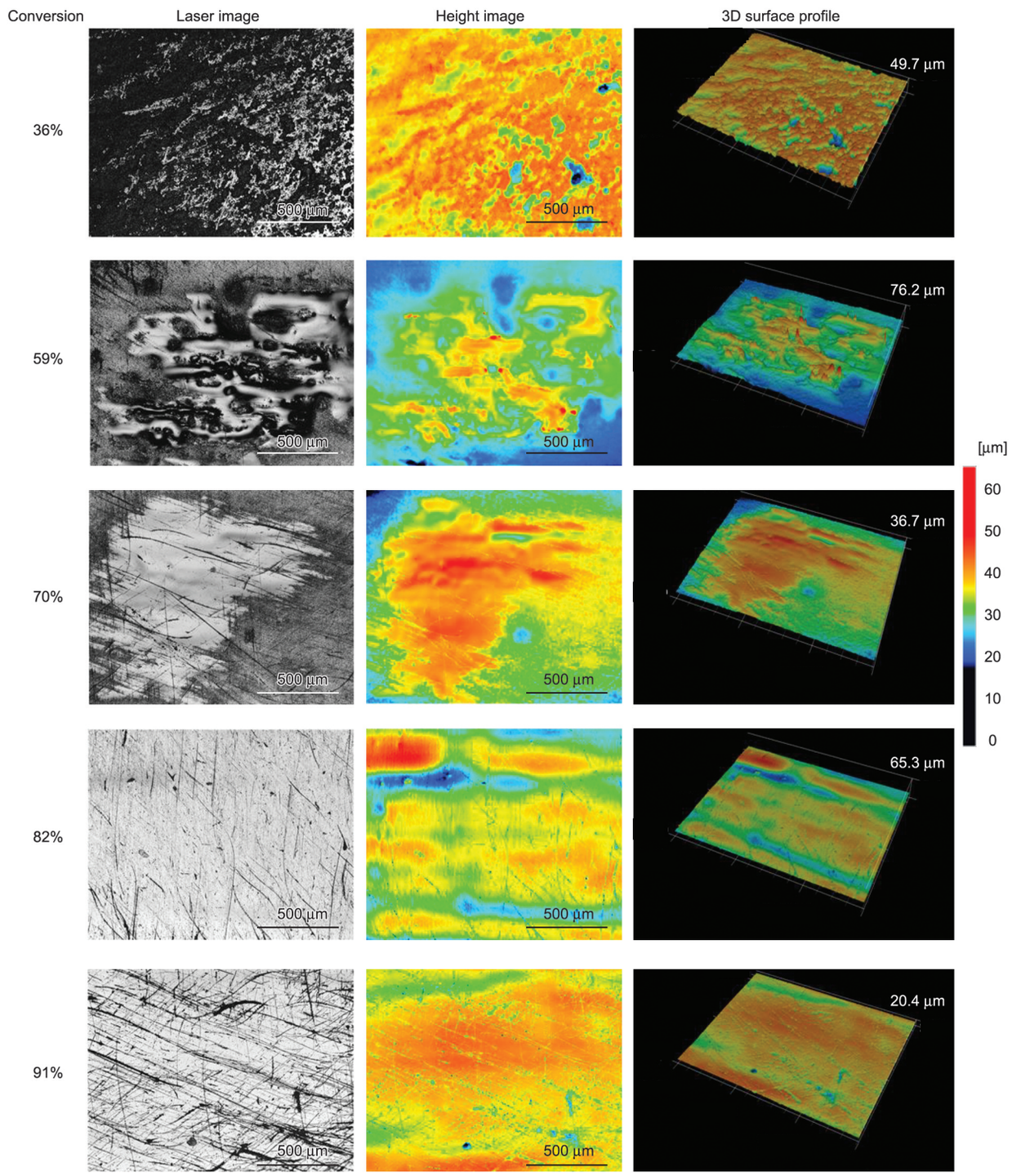

Figure 11. Topographical evaluation of the wear tracks for bio-based coatings with increasing degree of conversion (60 W/cm^2), including laser image, height image and 3D surface profile (all surface areas 1000×1500 µm^2 at magnification 100×, number on 3D scan represents max *z*-scale).

grooves that are not deformed and not smoothened. These observations are in agreement with the relatively high wear losses and the high microhardness of fossil-based coatings.

The detailed evaluation of wear tracks for bio-based coatings obtained with different degree of conversion is shown in Figure 11. A completely different morphology of the wear track for bio-based coating relatively to the fossil-based coatings is characterized through the formation of coating deposits in the wear track. The latter are irregularly formed lumpy deposits under weak curing conditions, but they gradually evolve over the formation of island-like deposits towards continuously smoothened films for the more severe curing conditions and higher degree of conversion. The latter are in parallel with the increase in mechanical properties and coherence of the polymerized network, forming a more homogeneous film. The latter is more ductile compared to the fossil-based coatings, which allows for deformation and smoothening along the wear track offering protection against severe abrasive wear.

4. Conclusions

In this study, the benefits of replacing traditional fossil-based acrylate coatings into bio-based acrylate coating grades were illustrated in terms of mechanical performance and physico-chemical properties. At present, however, possible differences in processing conditions and performance of bio-based coating grades may form a barrier to their widespread application.

The comparison of photochemical processing conditions for fossil- and bio-based coatings provided similar effects on the degree of conversion, depending on the photoinitiator concentrations, number of passes and UV light intensity. Under fully-cured conditions, bio-based coatings presented lower wear compared to fossil-based coatings. Alternatively, a remaining fraction of bio-based or fossil-based monomers adversely affected the abrasive wear properties, as the partially cured bio-based coatings provided steadily decreasing wear and fossil-based coatings showed increasing wear with high number of processing passes. The hardness of bio-based coatings was systematically lower than fossil-based coatings, which favorably reduced brittleness and abrasive wear. However, the wear behavior could not be fully explained through variations in bulk properties of the coating, as a regular evolution of hardness with processing conditions was noticed for partially cured coatings. Contrarily, the high hydrophobicity of bio-based coatings indicated the presence of a surface layer with additional lubricity. This was confirmed by examination of the wear tracks, showing brittle abrasive wear tracks for fossil-based coatings and film-like deposits for bio-based coatings. In particular, the ductility and hydrophobicity of bio-based coatings promoted better wear resistance.

In conclusion, the observations in this study provide vast evidence for a transition of fossil-based into bio-based coatings with similar processing properties and superior mechanical performance. Based on present results, the protective bio-based wood coatings may particularly find possible applications for indoor flooring and furniture application in the future.

References

[1] Pourhashem G.: Coating a sustainable future. Coatings, **10**, 713 (2020). https://doi.org/10.3390/coatings10080713

[2] Henn K. A., Forsman N., Zou T., Österberg M.: Colloidal lignin particles and epoxies for bio-based, durable, and multiresistant nanostructured coatings. ACS Applied Materials and Interfaces, **13**, 34793–34806 (2021). https://doi.org/10.1021/acsami.1c06087

[3] Teaca C. A., Roşu D., Mustaţă F., Rusu T., Roşu L., Roşca I., Verganici C. D.: Natural bio-based products for wood coating and protection against degradation: A review. BioResources, **14**, 4873–4901 (2019). https://doi.org/10.15376/biores.14.2.Teaca

[4] Hua, Q., Liu, L.Y., Karaaslan, M.A., Renneckar, S.: Aqueous dispersions of esterified lignin particles for hydrophobic coatings. Front. Chem. **7** (2019), 515. https://doi.org/10.3389/fchem.2019.00515

[5] Janesch J., Arminger B., Gindl-Altmutter W., Hansmann C.: Superhydrophobic coatings on wood made of plant oil and natural wax. Progress in Organic Coatings, **148**, 105891 (2020). https://doi.org/10.1016/j.porgcoat.2020.105891

[6] Nowrouzi Z., Mohebby B., Ebrahimi M., Petrič M.: Weathering performance of thermally modified wood coated with polyacrylate containing olive leaf extract as a bio-based additive. European Journal of Wood and Wood Products, **79**, 1551–1562 (2021). https://doi.org/10.1007/s00107-021-01712-3

[7] de Hoyos-Martinez P. L., Issaoui H., Herrera R., Labidi J., Charrier-El Bouhtoury F.: Wood fireproofing coatings based on biobased phenolic resins. ACS Sustainable Chemistry and Engineering, **9**, 1729–1740 (2021). https://doi.org/10.1021/acssuschemeng.0c07505

[8] Montazeri M., Eckelman M. J.: Life cycle assessment of UV-curable bio-based wood flooring coatings. Journal of Cleaner Production, **192**, 932–939 (2018). https://doi.org/10.1016/j.jclepro.2018.04.209

[9] Yu A. Z., Sahouani J. M., Webster D. C.: Highly functional methacrylated bio-based resins for UV-curable coatings. Progress in Organic Coatings, **122**, 219–228 (2018).
https://doi.org/10.1016/j.porgcoat.2018.05.035

[10] da Cruz M. G. A., Budnyak T. M., Rodrigues B. V. M., Budnyk S., Slabon A.: Biocoatings and additives as promising candidates for ultralow friction systems. Green Chemistry Letters and Reviews, **14**, 358–381 (2021).
https://doi.org/10.1080/17518253.2021.1921286

[11] Wu H., Liu C., Cheng L., Yu Y., Zhao H., Wang L.: Enhancing the mechanical and tribological properties of epoxy composites *via* incorporation of reactive bio-based epoxy functionalized graphene oxide. RSC Advances, **10**, 40148–40156 (2020).
https://doi.org/10.1039/D0RA07751H

[12] Akpan E. I., Wetzel B., Friedrich K.: A fully biobased tribology material based on acrylic resin and short wood fibres. Tribology International, **120**, 381–390 (2018).
https://doi.org/10.1016/j.triboint.2018.01.010

[13] Makshina E. V., Canadell J., van Krieken J., Peeters E., Dusselier M., Sels B.: Bio-acrylates production: Recent catalytic advances and perspectives of the use of lactic acid and their derivates. ChemCatChem, **11**, 180–201 (2018).
https://doi.org/10.1002/cctc.201801494

[14] Veith C., Diot-Néant F., Miller S. A., Allais F.: Synthesis and polymerization of bio-based acrylates: A review. Polymer Chemistry, **11**, 7452–7470 (2020).
https://doi.org/10.1039/D0PY01222J

[15] Liang B., Li R., Zhang C., Yang Z., Yuan T.: Synthesis and characterization of a novel tri-functional bio-based methacrylate prepolymer from castor oil and its application in UV-curable coatings. Industrial Crops and Products, **135**, 170–178 (2019).
https://doi.org/10.1016/j.indcrop.2019.04.039

[16] Voet V. S. D., Strating T., Schnelting G. H. M., Dijkstra P., Tietema M., Xu J., Woortman A. J. J., Loos K., Jager J., Folkersma R.: Biobased acrylate photocurable resin formulation for stereolithography 3D printing. ACS Omega, **2**, 1403–1408 (2018).
https://doi.org/10.1021/acsomega.7b01648

[17] Yuan M., Wang S., Li G., He S., Liu W., Liu H., Huang M., Zhu C.: UV curable hyperbranched polyester polyurethane acrylate for hydraulic machinery coating. Materials Research Express, **8**, 035104 (2021).
https://doi.org/10.1088/2053-1591/abecce

[18] Mashouf M., Ebrahimi M., Bastani S.: UV curable urethane acrylate coatings formulation: Experimental design approach. Pigment and Resin Technology, **43**, 61–68 (2014).
https://doi.org/10.1108/PRT-10-2012-0072

[19] Bednarczyk P., Nowak M., Mozelewska K., Czech Z.: Photocurable coatings based on bio-renewable oligomers and monomers. Materials, **14**, 7731 (2021).
https://doi.org/10.3390/ma14247731

[20] Lee B-H., Choi J-H., Kim H-J.: Coating performance and characteristics for UV-curable aliphatic urethane acrylate coatings containing Norrish type I photoinitiators. Journal of Coatings Technology and Research, **3**, 221–229 (2006).
https://doi.org/10.1007/BF02774511

[21] Li C., Cheng J., Chang W., Nie J.: Photopolymerization kinetics and properties of a trifunctional epoxy acrylate. Designed Monomers and Polymers, **16**, 274–282 (2013).
https://doi.org/10.1080/15685551.2012.747143

[22] Anastasio R., Peerbooms W., Cardinaels R., van Breemen L. C. A.: Characterization of ultraviolet-cured methacrylate networks: From photopolymerization to ultimate mechanical properties. Macromolecules, **52**, 9220–9231 (2019).
https://doi.org/10.1021/acs.macromol.9b01439

[23] Anastasio R., Cardinaels R., Peters G. W. M., van Breemen L. C. A.: Structure–mechanical property relationships in acrylate networks. Journal of Applied Polymer Science, **137**, 48498 (2019).
https://doi.org/10.1002/app.48498

[24] Kunwong D., Sumanochitraporn N., Kaewpirom S.: Curing behavior of a UV-curable coating based on urethane acrylate oligomer: The influence of reactive monomers. Songklanakarin Journal of Science and Technology, **33**, 201–207 (2011).

[25] Andrzejewska E.: Photopolymerization kinetics of multifunctional monomers. Progress in Polymer Science, **26**, 605–665 (2001).
https://doi.org/10.1016/S0079-6700(01)00004-1

[26] Liu J., Liu R., Zhang X., Li Z., Tang H., Liu X.: Preparation and properties of UV-curable multi-arms cardanol-based acrylates. Progress in Organic Coatings, **90**, 126–131 (2016).
https://doi.org/10.1016/j.porgcoat.2015.10.012

[27] Zhang H., Zhang H., Tang L., Zhang Z., Gu L., Xu Y., Eger C.: Wear-resistant and transparent acrylate-based coating with highly filled nanosilica particles. Tribololgy International, **43**, 83–91 (2010).
https://doi.org/10.1016/j.triboint.2009.05.022

[28] Wu J. F., Fernando S., Jagodzinski K., Weersasinghe D., Chen Z.: Effect of hyperbranched acrylates on UV-curable soy-based biorenewable coatings. Polymer International, **60**, 571–577 (2010).
https://doi.org/10.1002/pi.2980

[29] Patil D. M., Phalak G. A., Mhaske S. T.: Design and synthesis of bio-based UV curable PU acrylate resin from itaconic acid for coating applications. Designed Monomers and Polymers, **20**, 269–282 (2017).
https://doi.org/10.1080/15685551.2016.1231045

[30] Cogulet A., Blanchet P., Landry V.: Evaluation of the impacts of four weathering methods on two acrylic paints: Showcasing distinctions and particularities. Coatings, **9**, 121 (2019).
https://doi.org/10.3390/coatings9020121

[31] Andrzejewska E., Andrzejewski M.: Polymerization kinetics of photocurable acrylic resins. Journal of Polymer Science Part A: Polymer Chemistry, **36**, 665–673 (1997). https://doi.org/10.1002/(SICI)1099-0518(199803)36:4<665::AID-POLA15>3.0.CO;2-K

[32] Park Y-J., Lim D-H., Kim H-J., Park D-S. Sung I-K.: UV- and thermal-curing behaviors of dual-curable adhesives based on epoxy acrylate oligomers. International Journal of Adhesion and Adhesives, **29**, 710–717 (2009). https://doi.org/10.1016/j.ijadhadh.2009.02.001

[33] Tasic S., Bozic B., Dunjic B.: Synthesis of new hyperbranched urethane-acrylates and their evaluation in UV-curable coatings. Progress in Organic Coatings, **51**, 320–327 (2004). https://doi.org/10.1016/j.porgcoat.2004.07.021

[34] Huang L., Li Y., Yang J., Zeng Z., Chen Y.: Self-initiated photopolymerization of hyperbranched acrylates. Polymer, **50**, 4325–4333 (2009). https://doi.org/10.1016/j.polymer.2009.07.004

[35] Nguyen T. V., Nguyen-Tri P., Azizi T. S., Dang T. C., Hoang D. M., Hoang T. H., Nguyen T. L., Bui T. T. L., Dang V. H., Nguyen N. L., Le T. T., Nguyen T. N. L., Vu Q. T., Tran D. L., Dang T. M., Lu L. T.: The role of organic and inorganic UV-absorbents on photopolymerization and mechanical properties of acrylate-urethane coating. Materials Today Communications, **22**, 100780 (2020). https://doi.org/10.1016/j.mtcomm.2019.100780

[36] Oladele I. O., Ayanleye O. T., Adediran A. A., Makinde-Isola B. A., Taiwo A. S., Akinlabi E. T.: Characterization of wear and physical properties of pawpaw–glass fiber hybrid reinforced epoxy composites for structural application. Fibers, **8**, 44 (2020). https://doi.org/10.3390/fib8070044

[37] Choi J-H., Kim H-J.: Three hardness test methods and their relationship on UV-curable epoxy acrylate coatings for wooden flooring systems. Journal of Industrial Engineering and Chemistry, **12**, 412–417 (2006).

[38] Jiao Z., Wang X., Yang Q., Wang C.: Modification and characterization of urethane acrylate oligomers used for UV-curable coatings. Polymer Bulletin, **74**, 2497–2511 (2016). https://doi.org/10.1007/s00289-016-1847-4

[39] Barszczewska-Rybarek I. M.: A new approach to morphology studies on diacrylate polymer networks using X-ray powder diffraction. Macromolecular Chemistry and Physics, **214**, 1019–1026 (2013). https://doi.org/10.1002/macp.201200676

[40] Rey L., Duchet J., Galy J., Sautereau H., Vouagner D., Carrion L.: Structural heterogeneities and mechanical properties of vinyl/dimethacrylate networks synthesized by thermal free radical polymerisation. Polymer, **43**, 4375–4384 (2002). https://doi.org/10.1016/S0032-3861(02)00266-5

[41] Barszczewska-Rybarek I.: Structure-property relationships in dimethacrylate networks based on Bis-GMA, UDMA and TEGDMA. Dental Materials, **25**, 1082–1089 (2009). https://doi.org/10.1016/j.dental.2009.01.106

[42] Brighenti R., Cosma M. P.: Mechanical behavior of photopolymerized materials. Journal of the Mechanics and Physics of Solids, **52**, 104456 (2021). https://doi.org/10.1016/j.jmps.2021.104456

[43] Taki K., Nakamura T.: Effects of curing conditions and formulations on residual monomer contents and temperature increase of a model UV gel nail formulation. Journal of Cosmetics, Dermatological Sciences and Applications, **1**, 111–118 (2011). https://doi.org/10.4236/jcdsa.2011.14017S